RSC Advances

ROYAL SOCIETY OF CHEMISTRY

www.rsc.org/advances

Synthetic cobalt clays for the storage and slow release of therapeutic nitric oxide

Ana C. Fernandes[a]; Moisés L. Pinto[b], Fernando Antunes[a], João Pires[a]

[a] Centro de Química e Bioquímica, Faculdade de Ciências, Universidade de Lisboa, 1749-016 Lisboa, Portugal

[b] CERENA, Instituto Superior Técnico, Universidade de Lisboa, Av. Rovisco Pais, nº 1, 1049-001 Lisboa, Portugal

Abstract

Nitric oxide (NO) is one of the smallest endogenous molecules with particularly interesting aspects roles in biological systems, despite its toxicological potential. Solid carriers have potential biomedical interest in the delivery of exogenous NO for anti-bacterial, anti-thrombic and wound healing applications. In this work, a smectite clay was successful synthetized with incorporated cobalt ions in its structure, with the main goal of studying its potential in the field of storage and release of nitric oxide for therapeutic applications. Materials were characterized by X-ray diffraction, nitrogen adsorption at -196 ºC, TG-DSC and chemical analysis. The kinetic data for the nitric oxide storage and release was obtained in gas and in liquid phases. The released amounts of NO in the liquid phase were within the biological range and a slow release kinetics was obtained with, inclusively, an almost direct relation between the released fraction and time. Toxicological assays with HeLa cells indicated that the materials have low cytotoxicity.

Keywords: Synthetic clays, Cobalt-clays, nitric oxide, drug release

1. Introduction

Nitric oxide (NO) is one of the smallest endogenous molecules with particular interesting aspects on biological systems, despite its toxicological potential. The delivery of nitric oxide in controlled amounts in the human body is an attractive therapeutic alternative for a large number of pathologies. The various functions of NO include a neurological function in synaptic plasticity, neurotransmission, learning and memory, in addition to having a primary role in non-specific immunity and platelet aggregation inhibition.[1-7]

NO is a gas at normal temperature and pressure unlike more common drug molecules that are usually in solid or liquid state. Because of the limited utility of authentic NO gas in many experimental systems and the short half-life of NO in vivo, compounds that have the capacity to release NO slowly have been studied[8-11] Classic donors, usually based on diazeniumdiolates, are well established. The use of diazeniumdiolates in therapy is, however, limited because their action is systemic, that is, they become distributed throughout the body, thus compromising selectivity and causing unwanted side effects. Because of this multiplicity of effects, concentration control is very important, since exposures to high concentrations of NO are toxic. For example, several high-reactive toxic intermediates, such as dinitrogen trioxide and peroxynitrate, that react with biomolecules may be formed.[12, 13] In addition, many proteins contain transition metals that may react with NO leading in the inhibition of their function, which may result in toxicity.[14]

The growth of interest in the physiology of NO since the mid-1980s[6] has led to the development of a variety of new NO donors that offer several advantages over conventional NO donors. In this context, solid carriers have biomedical interest in the delivering of exogenous NO. Initial research on materials for NO storage was

concentrated on polymeric nanoparticles matrix.[8] Zeolites were also studied and presented a delivery capacity similar to the best polymers.[9, 15, 16] Metal–organic frameworks (MOFs) were studied in this context.[8, 15-18] Clays have also been studied in this context.[11, 19, 20]

Clays and clay minerals play an important role in the field of health products. In fact, they are fundamental components in several medical products, being used as excipients and fulfilling some technological functions. Particularly relevant in the context of adsorption are the 2:1 clays minerals, such as smectites because these are expandable materials. Smectites are formed by one sheet of cations (usually Al^{3+}, Fe^{2+}, Fe^{3+} or Mg^{2+}) in octahedral coordination sandwiched between two sheets of cations (usually Si^{4+} or Al^{3+}) in tetrahedral coordination with the oxygen atoms.[21] The structure of the 2:1 layered clays is schematically exemplified in Fig. S1 in Electronic Supplementary Information. In addition, clay minerals may be effectively used in the development of new drug delivery systems, being a potential vehicle to store and release NO.[11, 19, 20, 22, 23] Good adsorption capacity is not the only requirement for a NO-delivery material. An appropriate releasing kinetics is also of paramount importance to maintain a given concentration in the surrounding environment. In general, a slow-releasing kinetics is preferred because it allows for easier and safer control of the NO concentration for longer periods. Additionally, and not of least importance, to be used in drug delivery a material must be biocompatible. Modified clays have been studied with good results. [11, 19, 20]

In the present work, we synthetized smectite clays with cobalt ions incorporated in its structure. The main objectives of preparing these synthetic clays were twofold. Firstly, cobalt is not usually present in natural clays but this metal is of particular interest due to its capability of coordinating NO[24, 25] and its low toxicity. Secondly,

being synthetic materials it will be in principle possible to obtain samples with more uniform, and preferentially smaller, particle dimensions than what occurs in natural clays, which is an aspect that is related with certain types of applications for NO delivering materials.

2. Experimental

2.1. Preparation of the Cobalt Clays

Cobalt clays, with two different silicon sources, silicic acid (99.9 %, < 20 μm Sigma- Aldrich) and tetramethyl orthosilicate, TMOS (36.5-38 %, Sigma-Aldrich) were prepared by hydrothermal treatment of mixtures with cobalt chloride ($CoCl_2.6H_2O$, *p.a.*, Sigma Aldrich) and NaOH (98%, BDH Chemicals Ltd), using a procedure adapted from the literature.[26-28]

The synthesis with silicic acid had two strands:

A) 8 mL of 2 M NaOH were added, dropwise under, to a mixture of $CoCl_2 \cdot 6H_2O$ (0.7 g) in 100 mL of 45 mM silicic acid and $Na_2S_2O_4$ (1 g, Sigma-Aldrich) under N_2. This gave a light pink cobalt hydroxide suspension. After 2 days stirring at room temperature, in a closed flask, it was transferred to an autoclave, and left in the oven at 150 °C for 50 h. The sample obtained was named CoAS-A.

B) 12.5 mL of 2 M NaOH were added, dropwise to a solution of $CoCl_2 \cdot 6H_2O$ (1.21 g) in 150 mL of water under N_2. This gave a light pink cobalt hydroxide suspension. After 7 hours, silicic acid (0.65 g) and $Na_2S_2O_4$ (1 g) were added, and the mixture was stirred overnight under N_2. The mixture was then transferred to an autoclave, and heated at 150 °C for 50 h. The sample obtained was named CoAS-B. After this initial part, the procedure was the same for both samples, CoAS-A and CoAS-B. The suspensions were centrifuged, washed and left stirring in 1 M NaCl solution

overnight. The materials were then washed with distilled water, dialyzed through cellulose membranes (Sigma-Aldrich), and dried.

For the sample prepared with TMOS, named CoOS, the procedure was the same as the one used A) strand, as described for CoAS-A, only changing the silicon source.

The prepared materials were then characterized and compared with a natural smectite, montmorillonite (from Wyoming, USA). Montmorillonite is a 2:1 clay, meaning that it has two tetrahedral sheets of silica sandwiching a central octahedral sheet of alumina. The particles are plate-shaped with an average diameter below 2 μm and a thickness of 0.96 nm. This clay exhibits unique properties such as intercalation, swelling, and strong adsorption, and it also has been applied in some biotechnological and biomedical studies. [11, 20, 29-32]

2.2. Characterization methods

The products were characterized by powder X-ray diffraction (XRD), FT-IR, scanning electron microscopy (SEM), TG-DSC, and N_2 Adsorption at -196 °C.

Powder X-ray diffraction (XRD) patterns were recorded on a Philips PW 1730 diffractometer with automatic data acquisition (APD Phillips (v3.6B) software using a CuK_α radiation (λ=1.5406 Å)). Diffractograms were obtained from 5 to 50 and 4 to 16 2Θ/ º, with a step size of 0.017 2θ / º, and time per step of 100 s. Oriented mounts were obtained by covering a glass microscope slide with a suspension of sample in water (previously dispersed in an ultrasonic bath for 5 minutes), and then placed in an oven at 50 °C and left to dry. Glycolation, to determine if the products were swelling clays, was done by heating the oriented mounts in a sealed flask containing ethylene glycol at 90 °C for 5 h.[33]

Diffuse reflectance spectroscopy (DRIFTS) was recorded at room temperature using a Nicolet 6700 Fourier Transform IR spectrophotometer with data acquisition software OMNIC 7.2 (256 scans, resolution of 4 cm^{-1}) in the range of 400-4000 cm^{-1} Samples were analyzed in powder, diluted with KBr.

Chemical analysis of cobalt contents were obtained by atomic absorption spectroscopy of digested samples using a Unicam 929 (ATI UNICAM) spectrophotometer. Dynamic Light Scattering (DLS) analysis was performed using a Zetasizer Nano ZS from Malvern Instruments, to measure the hydrodynamic diameter (HD). For the HD measurement, the samples dispersed in water (0.5 mg cm^{-3}) were stirred for 5 minutes in an ultrasonic bath. DLS plots of are number averaged. Nitrogen (Air Liquid, 99.999%) adsorption isotherms were measured in a volumetric automatic apparatus (Micromeritics, ASAP 2010), at − 196 °C using a liquid nitrogen cryogenic bath. The samples, between 50 and 100 mg, were outgassed for 2.5 h, at a pressure lower than 0.133 Pa, at 250 °C.

2.3. Nitric Oxide adsorption and release

The kinetic adsorption profiles of NO in the synthetized materials were determined in a microbalance (C. I. Electronics, Disbal) suited for vacuum, connected to a high-vacuum pump system composed of a turbomolecular pump and a diaphragm pump (Pfeiffer Vacuum). Adsorption studies were made in gas phase, where samples were outgassed in the same conditions as for nitrogen adsorption experiments and release studies were performed both in gas and liquid phase. NO was introduced in the system until an 80 kPa pressure was attained. The microbalance was connected to a computer and the weight was recorded at fixed time intervals of 2 points per minute, for 72 h or equilibrium. After this period of time, vacuum was made in the cell and NO

release started, the weight decreasing was recorded for 48 h maximum. Pressure readings were made with a capacitance transducer (Pfeiffer Vacuum, CMR 262). The temperature was controlled at 25 °C using a water bath (Grant, GD120), with 0.05 °C precision.

The release studies were also performed in the liquid phase, following the Oxyhemoglobin Assay, described in the literature[34]. This method is based on the reaction of oxyhemoglobin with NO to form methemoglobin. As it is well known, in the presence of even minor amounts of oxygen in aqueous solution, NO is highly unstable. Therefore, to accurately determine the NO amount, the reaction of the detector with the NO must be more rapid than that of other competing species. In the oxyhemoglobin assay, this prerequisite is met due to the high rate of reaction between NO and oxyhemoglobin, which has been estimated to be at least 26 times faster than the autoxidation of NO in aqueous solution (even under saturating oxygen concentrations)[34]. The advantage of the rapid reaction between NO and oxyhemoglobin is obvious in that the trapping of NO by oxyhemoglobin will be almost stoichiometric under most experimental conditions. Therefore, the oxyhemoglobin assay is somewhat unique among methods for NO determination, as it is less subject to constraints imposed by competing reactions with oxygen or other reactants. To avoid dispersion problems of the samples in the liquid phase, those were ground with poly(tetrafluoroethylene) (PTFE, 25 mm particle size powder, from Aldrich) in a weight proportion of 75:25 (sample:PTFE). The mixture was then pressed into disks (5 mm diameter), under 8 tons for 30 s. Then, 6 mg of the disks were introduced into small glass crucibles in vacuum glass cells with a PTFE vacuum valve. The cells were connected to a vacuum line and samples were degassed in vacuum for 2.5 h hours, at 250 °C. NO was introduced into the cells and the pressure allowed to stabilize at 80 kPa. The valve was closed and the

sample left in contact with NO for 72 hours. The cell was then evacuated for one minute and filled with helium up to atmospheric pressure. The cell was closed and removed from the vacuum line. For the NO release, the cell was opened, the crucible removed and the pellet was added to 3 mL of oxyhemoglobin solution (1 μM) in a quartz container, which was vigorously shaken and the measurements started. The spectra of the solutions were taken at 10 minute intervals during 2 h, using a UV/vis spectrophotometer (Genesys 10S UV-Vis Spectrophotometer from Thermo Scientific). Prior to this, oxyhemoglobin solution was prepared by dissolving 20 mg of lyophilized human hemoglobin in 1 mL of 0.1 M phosphate buffer (pH=7.4). Purification and desalting were performed by passing the resulting oxyhemoglobin solution over a column of Sephadex G-25.[34]

2.4. Cell culture

HeLa cells (American Type Culture Collection, Manassas, VA, USA) were cultured at 37 °C in a humidified atmosphere with 5% CO_2. Cell culture medium consisted of RPMI-1640 supplemented with 10 % of fetal calf serum (FBS), 5 mL of L-Glutamine and 5 mL of antibiotics from Life Technologies.

2.5. Toxicological essays

Cells were plated in 96-well microplates (Orange Scientific) with 7500 and 2500 cells/well (for 24 h and 72 h sample assay, respectively) in a final volume of 100 μL cell culture media.

After 24 h incubation 10 μL of each sample was added to eight different wells. Before the experiment, the medium was removed and replaced by 100 μL/well of fresh new medium. Then 10 μL of alamarBlue® was added directly to each well, the

microplates were incubated at 37 °C for 4 h and the fluorescence signal was measured (nine measures/well) on a Spectra Max Gemini EM from Molecular Devices, with a SoftMax Pro software. Three independent experiments were taken for each sample. Cell viability was calculated by the following equation:

$$Cell\ viability\ = (\frac{F_{sample}}{F_{control}})$$

where F_{sample} is the fluorescence of the cells incubated with samples and $F_{control}$ is the fluorescence of the cells incubated without the sample. For CoAS-A a concentration study was made. In this case, CoAS-A concentration varied between 113 and 1800 µg/mL. Survival was evaluated, after 24 h, as described above. In preliminary experiments, it was observed that our test compounds did not affect alamarBlue® fluorescence. Images of the cell cultures were obtained in an optical phase-contrast microscope (Olympus CK40).

3. Results and discussion

3.1. Characterization of the samples

Fig. 1 shows the powder X-ray diffraction patterns obtained for cobalt materials. The samples gave reflections similar to montmorillonite (MMT), with basal spacing, before and after glycolation, as depicted on Table 1.

After exposure to ethylene glycol vapors the basal spacing increased and decreased after the samples were heated at 300 °C (Fig. 2), a behavior characteristic of swelling smectites clays. Besides MMT, the sample CoAS-A was the material where the swelling was better observed. The synthetic materials have smaller particle size than MMT, as discussed below, being this the most probable reason for the experimental

difficulty in the preparation of the oriented mounts and hence to the worst definition of the diffractograms in some samples, particularly for sample CoAS-B (not shown) .

As determined by chemical analysis, the cobalt ions content on the samples were of 9 % for the sample prepared with TMOS (CoOS) and 22 and 30 % for samples prepared with silicic acid (CoAS-A and CoAS-B, respectively).

Fig. 3 presents the infrared spectra for the synthesized materials and for montmorillonite. For the latter, the characteristic silicate bands can be observed: the stretching vibration of Si-O-Si group occur between 1027 and 1091 cm^{-1}; in the region between 400 and 800 cm^{-1} are observed various vibration stretching which correspond to the links Si-O-M groups (M = aluminum, magnesium and other metals present in the clay). In addition, a band could be observed next to 3625 cm^{-1} attributed to the stretching vibrations of the -OH groups. The absorption at approximately 3434 cm^{-1} can be attributed to the OH group stretching vibrations related to the adsorbed water with the corresponding deformation vibrations of water observed at 1621 cm^{-1}.

All the synthesized materials, present the stretching vibration of Si-O-Si bond (1027-1091 cm^{-1}), although with different intensity. The bands corresponding to Si-O-M vibrations, that occur around 400-800 cm^{-1}, are also present in all samples; in this case, it may correspond to links with cobalt ions (Si-O-Co). The vibrations corresponding to the stretching of the OH groups (3600 cm^{-1}) are present, as well as the typical vibrations of stretching and deformation of the OH groups of adsorbed water, 3400 cm^{-1} (except for the CoAS-A sample).

The characterization results for the synthesized materials carried out by XRD and FT-IR, as discussed above, are compatible to the existence of expandable smectite type clay materials.

DLS is a versatile and useful technique for measuring the particle size distributions. It should be emphasized that in DLS analysis it is considered that the particles have a spherical shape, so the results in the materials studied here need to be interpreted with due reservations, admitting however the comparative analysis which was carried out between the various materials. Thus, in Fig. 4, it is noted that the CoOS material has a particle size distribution between 100 and 250 nm, having, on average, its particle size is around 200 nm. The sample CoAS-A shows an average particle size distribution shifted to higher values, of about 400 nm, but still having particles between 1500 and 2500 nm resulting from particle aggregation. The CoAS-B material has particles with sizes mostly of 100 and 450 nm, and its particle size distribution is very similar to the CoOS sample. The CoAS-B sample, however, also tends to form aggregates with sizes between 500 and 1000 nm approximately. It must be emphasized that the particle size distributions of the synthetic cobalt clays prepared in this work reveal particle sizes that are considerably lower, and for the CoOS sample the distribution itself is narrower, than those found for the natural montmorillonite clay (MMT). This points out the potential of the synthetic clays for not only topical deliver of NO but also for intracorporeal applications since the dimensions of the particles are well below the dimensions of the capillar blood vessels which have radius of 4 μm or higher.[35]

The nitrogen adsorption-desorption isotherms at -196 ºC for CoAS-B, such as for MMT, can be classified as type IIb[36] (Fig. 5) as expected for raw clays, which are non-porous materials composed of aggregates of plate-like particles. The samples, CoAS-A and CoOS, exhibit similar isotherms between each other, with mixed features of type I and IV. [37] [36] From the nitrogen adsorption data, the surface area, A_{BET}, was determined (Table 2). Below 0.4 p/p^0, that is, at relative pressure range where the

adsorption in the micropores is complete but capillary condensation in mesopores (pore width between 2 and 50 nm) has not started, CoAS-A and CoOS are the materials which adsorb the most, presenting the highest A_{BET} values. The extension of the hysteresis loops is similar for the various materials but is smaller for CoAS-B which is the material more similar to MMT, presenting, although higher surface area (A_{BET}) than MMT.

Both CoSA-A and CoOS, present a much higher surface area (A_{BET}) values as well as an increase of microporous volume (Table 2). The large surface area (A_{BET}), for CoAS-A and CoOS, is probably due to its morphology and the smaller particle size as already mentioned. These materials, being considered as unmodified clays, present a surface area comparable to some pillared clay materials previously studied.[11, 19]

From the data in Fig. 5 the pore size distributions were determined by DFT method – Fig. 6. Unlike montmorillonite (non-porous), CoAS-A and CoOS materials present microporosity with wide pores around 1.5 nm and also mesoporosity with pore width in a range of 2 to 10 nm. CoAS-B material, do not present microporosity, being essentially mesoporous.

3.2. Nitric Oxide adsorption and release

Data for adsorption and release, in the gas phase, of nitric oxide is shown in Fig. 7 a) and b), respectively. As can be seen in Fig. 7 a), the synthetic clays adsorb higher amounts of nitric oxide comparing with montmorillonite.

NO adsorbed amounts for the cobalt samples were between 3.5 % (CoAS-B) and 5.1 % (CoOS) in mass (Table 3). The latter material presented a value similar to what was found for instance for type-A zeolites[9] and for pillared clays[11, 19]. The adsorption kinetics was initially fast, decreasing with time. As can be seen in Fig. 7 b), the samples

released between 30 to 40 % of the adsorbed nitric oxide. The release kinetics was also faster on the two first hours, with almost 60 % of NO being released during that period of time.

NO released from the synthetic clays was assessed in liquid phase from the spectral changes of hemoglobin solutions in contact with the loaded solids – Fig. 8 a) b) c) – as described in the experimental section. Comparing the initial spectrum and the spectrum obtained after 2 hours, when using CoAS-A, a slight decrease in the intensity of the 542 and 577 nm absorption bands was observed. Also, there was a slight shift to lower wavelengths from the 415 nm band. This indicates that the sample released low amounts of nitric oxide.

When comparing the UV-Vis spectrums of the oxyhemoglobin solution after 2 hours contact with CoOS and CoAS-B, the changes were evident and correspond to the transformation of oxyhemoglobin to methemoglobin. Comparing the initial spectrum and the spectrum obtained after 2 hours, a decrease in the intensity of the 542 and 577 nm absorption bands was observed, indicating the consumption of oxyhemoglobin. The appearance of the 500 and 630 nm bands shows the formation of methemoglobin with NO[34]. Also, in accord with the transformation of the oxyhemoglobin to methemoglobin is the shift to lower wavelengths of the band at 415 nm.

The release of nitric oxide, from the synthetic clays, in the hemoglobin solution, was followed during time. The release profiles are depicted on Fig. 9 in the form of nitric oxide concentration *versus* time, and the maximum released amounts can be found in **Error! Reference source not found.**.

The NO amounts released in liquid phase are not entirely in line with the results obtained in gas phase. In gas phase both materials prepared from silicic acid released similar amounts of NO, being the ones which released the most. In liquid phase,

however, these same materials present a huge difference regarding the NO amounts released. The sample CoAS-B released significantly more NO than CoAS-A. The release for CoAS-A was linear with time, and almost linear for the sample CoOS. The material CoAS-B presented a faster release in the first hour experiment, and then begun to slower and tends to a plateau.

To better understand the results obtained, NO release data was analyzed according to Higushi, $M/M_0 = kt^{1/2}$ (1), Korsmeyer et al., $M/M_0 = kt^n$ (2) and Peppas and Sahlin, $M/M_0 = k_d t^m + k_r t^{2m}$ (3) equations,[38-41] where M/M_0 is the drug released fraction at time t, k is the kinetics constant characteristic of NO / clay system, n is the release exponent that depends on the release mechanism and the shape of the matrix tested, k_d and k_r are the diffusion and relaxation rate constants, respectively, m is the purely Fickian diffusion exponent for a device of any geometrical shape which exhibits controlled release.[38, 39] Regression parameters were determined using OriginPro 8.5 software. Since models from equations (1) to (3) have a different number of adjustable parameters the Akaike's Information Criterion (AIC)[42] instead of the regression coefficient (R^2) was used to determine the best fitting model.

For better comparison of the release kinetics the fractional released, expressed by M/M_0 were M an M_0 are the concentrations at a given time and 2 h, respectively, is shown in Fig. 10.

According to the AIC method the equation to be used for the releasing, when using CoAS-B and CoOS is the Peppas-Sahlin, evidencing that the release follows two mechanism: diffusion and relaxation, while using CoAS-A the Korsmeyer-Peppas is the model which better applied. In Table 5 can be found the constant release values for all the prepared materials as well as for MMT, obtained in previous works.[11] For the materials CoAS-B and CoOS the relaxation parameter took negative values, however,

these values are very close to zero so they can be considered only residual. Its diffusional kinetic parameters are very similar; being lower than the one of MMT, which is an advantage in the present context as the goal is a slow release. CoAS-A material followed the Korsmeyer-Peppas model, evidencing the prevalence of a Fickian diffusional release that occurs by the usual molecular diffusion due to a chemical potential gradient.[41] It is the material with the lower kinetics constant, and as mentioned above the sample for which the relation between the NO released and time is more linear. For all the materials the release cannot be considered purely Fickian, as the release exponent (n) is higher than 0.5.

3.3. Toxicological essays

Taking into account the obtained results, namely, NO amounts adsorbed/released as well as the release kinetics parameter, toxicological assays were carried out for all the three samples. The toxicity of the materials was studied using HeLa cells and a material concentration of 450 μg/mL, by measuring the survival after 24 and 72 hours – Fig. 11. For all the materials, the results indicated a survival rate of at least 80% after 24h, being above 90 % for CoAS-A and CoOS. After 72h exposition, the viability tended to decrease, being more significantly for CoOS.

These results, in the overall indicate a low cytotoxicity (except for CoOS at 72 h exposure) because a 450 μg/mL concentration is in the high end of the range usually tested for porous material.[43-49] Considering the preliminary toxicity studies and the results of NO releasing in liquid phase, the samples CoAS-A and CoOS were selected for a study of the survival rate in which the concentration of the solid was varied – Fig. 12.

It is evident that for the CoOS sample the cell viability tends to decrease with the increase in sample concentration, but still is above 50 % for the highest concentration. For the CoAS-A material, in the overall, viability remained high in all range of concentrations. These results are better than the ones found for other natural clays as montmorillonite[20] and Sepiolite[19].

4. Conclusions

The synthetic clays prepared in this work not only possessed high surface area, and low particle size distributions, but also were able to adsorb higher amounts of nitric oxide than a natural smectite clay. The released amounts of nitric oxide were also higher (about four times) than for the natural clay and, particularly in liquid phase, the release tends to be slow and linear with the time. It is evident that the presence of cobalt metal centers in the synthetic clays improves the NO storage capacity. The cytotoxicity studies with HeLa cells indicated a survival of at least 70 % after 24 and 72 hours (with exception for CoOS sample at 72 h), which is an excellent result, considering the high concentration of material used on the tests. In overall the results are an encouraging indication that therapeutic applications involving NO release are a possibility for these type of materials.

Acknowledgments

We thank the Foundation for Science and Technology for funding CQB UID/MULTI/00612/2013 and CERENA UID/ECI/04028/2013 and for the grant

SFRH/BD/72058/2010 (ACF). MPL thanks for the Investigador FCT contract (IF/00993/2012).

References

1 S. Moncada, *Journal of the Royal Society of Medicine*, 1999, **92**, 164-169.
2 P. Sonveaux, B. F. Jordan, B. Gallez and O. Feron, *European journal of cancer (Oxford, England : 1990)*, 2009, **45**, 1352-1369.
3 A. Ghaffari, D. H. Neil, A. Ardakani, J. Road, A. Ghahary and C. C. Miller, *Nitric Oxide*, 2005, **12**, 129-140.
4 E. Karpuzoglu and S. A. Ahmed, *Nitric Oxide*, 2006, **15**, 177-186.
5 C. Napoli and L. J. Ignarro, *Annual Review of Pharmacology and Toxicology*, 2003, **43**, 97-123.
6 L. J. Ignarro, G. M. Buga, K. S. Wood, R. E. Byrns and G. Chaudhuri, *Proceedings of the National Academy of Sciences of the United States of America*, 1987, **84**, 9265-9269.
7 L. J. Ignarro, C. F. Napoli and J. Loscalzo, *Circ Res*, 2002, **90**, 21-28.
8 R. E. Morris and P. S. Wheatley, *Angew. Chem.-Int. Edit.*, 2008, **47**, 4966-4981.
9 P. S. Wheatley, A. R. Butler, M. S. Crane, S. Fox, B. Xiao, A. G. Rossi, I. L. Megson and R. E. Morris, *J. Am. Chem. Soc.*, 2006, **128**, 502-509.
10 M. L. Pinto, A. C. Fernandes, J. Rocha, A. Ferreira, F. Antunes and J. Pires, *Journal of Materials Chemistry B*, 2014, **2**, 224-230.
11 A. C. Fernandes, M. L. Pinto, F. Antunes and J. Pires, *Journal of Materials Chemistry B*, 2013, **1**, 3287.
12 J. S. Beckman, in *Nitric Oxide*, ed. J. Lancaster, Academic Press, San Diego, 1996, pp. 1-82.
13 P. Calcerrada, G. F. Peluffo and R. Radi, *Curr Pharm Des*, 2011, **17**, 3905-3932.
14 L. K. Keefer, *Nat Mater*, 2003, **2**, 357-358.
15 N. J. Hinks, A. C. McKinlay, B. Xiao, P. S. Wheatley and R. E. Morris, *Microporous and Mesoporous Materials*, 2010, **129**, 330-334.
16 R. E. Morris, N. J. Hinks, A. C. McKinlay, B. Xiao and P. S. Wheatley, *Microporous and Mesoporous Materials*, 2009.
17 P. Horcajada, R. Gref, T. Baati, P. K. Allan, G. Maurin, P. Couvreur, G. Férey, R. E. Morris and C. Serre, *Chemical Reviews*, 2012, **112**, 1232-1268.
18 A. C. McKinlay, B. Xiao, D. S. Wragg, P. S. Wheatley, I. L. Megson and R. E. Morris, *J. Am. Chem. Soc.*, 2008, **130**, 10440-10444.
19 A. C. Fernandes, F. Antunes and J. Pires, *New Journal of Chemistry*, 2013, **37**, 4052.
20 A. C. Fernandes, M. L. Pinto, F. Antunes and J. Pires, *Journal of Materials Chemistry B*, 2015, **3**, 3556-3563.
21 M. F. Brigatti, E. Galán and B. K. G. Theng, in *Handbook of clay science Part A: Fundamentals*, eds. F. Bergaya and G. Lagaly, Elsevier, Amsterdam, 2nd edn., 2013.
22 V. Anand, R. Kandarapu and S. Garg, *Drug Discovery Today*, 2001, **6**, 905-914.
23 P. C. C. Viseras, R. Sanchez, I. Salcedo, C. Aguzzi, *Applied Clay Science*, 2010, **48**, 291-295.
24 K. Tsuji, M. Imaizumi, A. Oyoshi, I. Mochida, H. Fujitsu and K. Takeshita, *Inorganic Chemistry*, 1982, **21**, 721-725.
25 H. Praliaud, G. F. Coudurier and Y. B. Taarit, *Journal of the Chemical Society, Faraday Transactions 1: Physical Chemistry in Condensed Phases*, 1978, **74**, 3000-3007.
26 G. V. Yan Xiang, *Clays and Clay Minerals*, 1996, **44**, 515-521.

27 Y. F. Tadashi Mizutani, Akane Okada, Osami Kamigaito, Takayuki Yashi, *Clays and Clay Minerals*, 1991, **39**, 381-386.

28 B. Scott, J. Crouse, M. Correia, L. Sun and G. Villemure, *Applied Clay Science*, 2010, **48**, 46-54.

29 H. H. Murray, *Clay Minerals*, 1999, **34**, 39-49.

30 D. Songurtekin, E. E. Yalcinkaya, D. Ag, M. Seleci, D. O. Demirkol and S. Timur, *Applied Clay Science*, 2013, **86**, 64-69.

31 B. Wicklein, M. Darder, P. Aranda and E. Ruiz-Hitzky, *Langmuir*, 2010, **26**, 5217–5225.

32 M. S. Lakshmi, M. Sriranjani, H. B. Bakrudeen, A. S. Kannan, A. B. Mandal and B. S. R. Reddy, *Applied Clay Science*, 2010, **48**, 589–593.

33 A. P. F. Albers, F. G. Melchiades, R. Machado, J. B. Baldo and A. O. Boschi, *Cerâmica*, 2002, **48**, 34-37.

34 D. K. Martin Feelisch, Jürgen Werringloer, in *Methods in Nitric Oxide Research*, ed. M. F. a. J. S. Stamler, John Wiley & Sons Ltd, First edn., 1996, p. 732.

35 J. A. Ritter, A. D. Ebner, K. D. Daniel and K. L. Stewart, *Journal of Magnetism and Magnetic Materials*, 2004, **280**, 184-201.

36 F. Rouquerol, J. Rouquerol and K. Sing, *Adorption by powders porous solids*, Academic Press, London, 1999.

37 K. S. W. Sing, D. H. Everett, R. A. W. Haul, L. Moscou, R. A. Pierotti, J. Rouquerol and T. Siemieniewska, *Pure & Appl. Chem.*, 1985, **57**, 603-619.

38 J. Siepmann and F. Siepmann, *Journal of Controlled Release*, 2012, **161**, 351-362.

39 Y.-S. Lin, Graduate School of the UniversityMinnesot, 2012.

40 C. Ferrero, I. Bravo and M. R. Jiménez-Castellanos, *Journal of Controlled Release*, 2003, **92**, 69-82.

41 N. A. Peppas and J. J. Sahlin, *International Journal of Pharmaceutics*, 1989, **57**, 4.

42 H. J. Motulsky and A. Christopoulos, *Fitting Models to Biological Data using Linear and Nonlinear Regression. A practical guide to curve fitting.*, GrapfPad Software, Inc, San Diego CA, 2003.

43 B. D. Kevadiya, R. P. Thumbar, M. M. Rajput, S. Rajkumar, H. Brambhatt, G. V. Joshi, G. P. Dangi, H. M. Mody, P. K. Gadhia and H. C. Bajaj, *European Journal of Pharmaceutical Sciences*, 2012, **47**, 265-272.

44 N. Venkatesan, J. Yoshimitsu, Y. Ito, N. Shibata and K. Takada, *Biomaterials*, 2005, **26**, 7154-7163.

45 S. W. Song, K. Hidajat and S. Kawi, *Langmuir*, 2005, **21**, 9568-9575.

46 M. F. Calmon, A. T. de Souza, N. M. Candido, M. I. B. Raposo, S. Taboga, P. Rahal and J. G. Nery, *Colloids and Surfaces B: Biointerfaces*, 2012, **100**, 177-184.

47 A. Bogershausen, S. J. Pas, A. J. Hill and H. Koller, *Chem. Mat.*, 2006, **18**, 664-672.

48 F. Y. Qu, G. S. Zhu, S. Y. Huang, S. G. Li, J. Y. Sun, D. L. Zhang and S. L. Qiu, *Microporous and Mesoporous Materials*, 2006, **92**, 1-9.

49 A. F. Peixoto, A. C. Fernandes, C. Pereira, J. Pires and C. Freire, *Microporous and Mesoporous Materials*, 2016, **219**, 145-154.

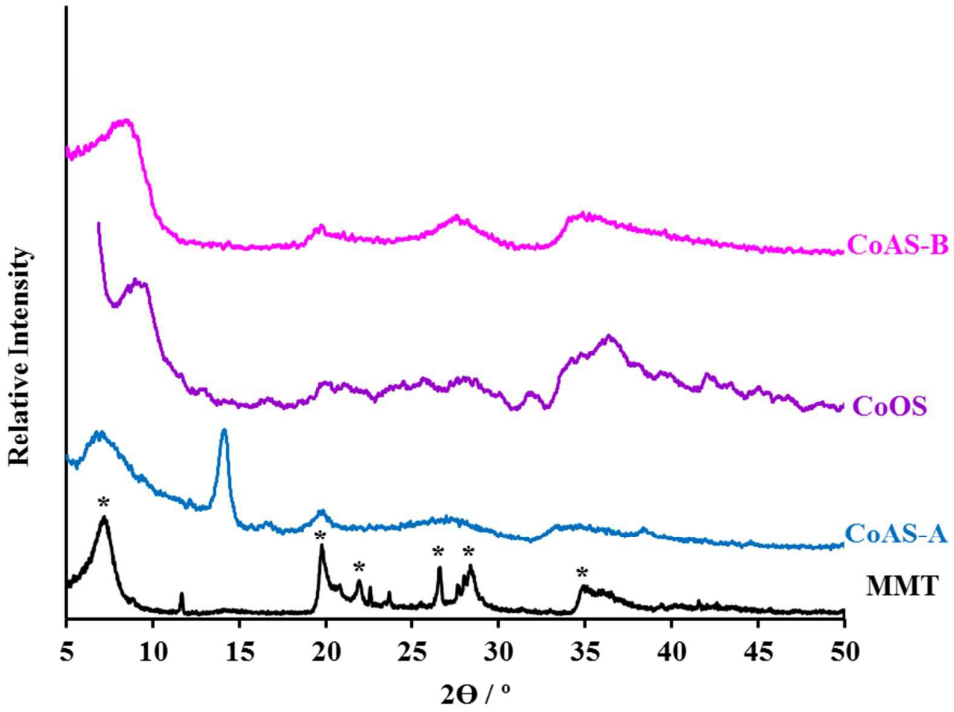

Fig. 1 DRX curves for montmorillonite and synthetic clays materials.

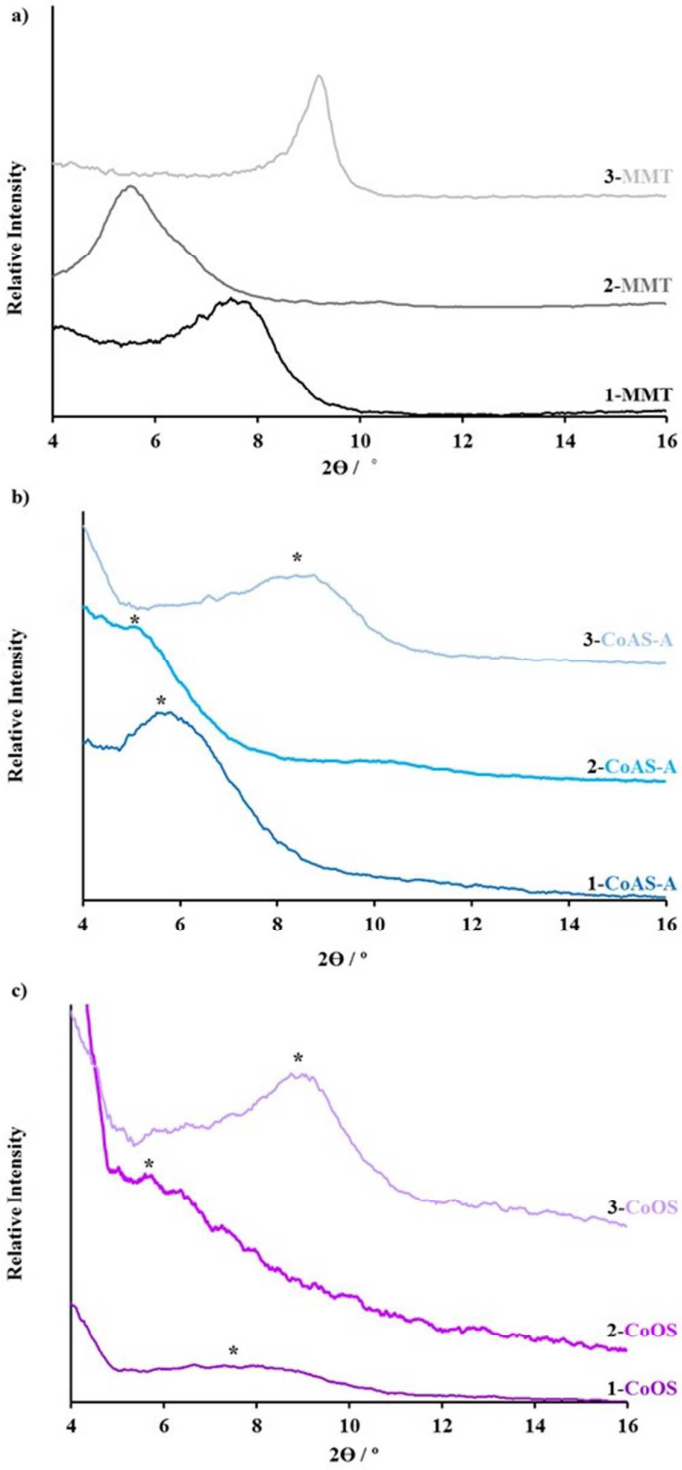

Fig. 2 DRX curves for a) montmorillonite, b) CoAS-A, c) CoOS. 1 – Dry sample; 2 – after exposure to ethylene glycol vapors; 3 – After heating at 300 ºC.

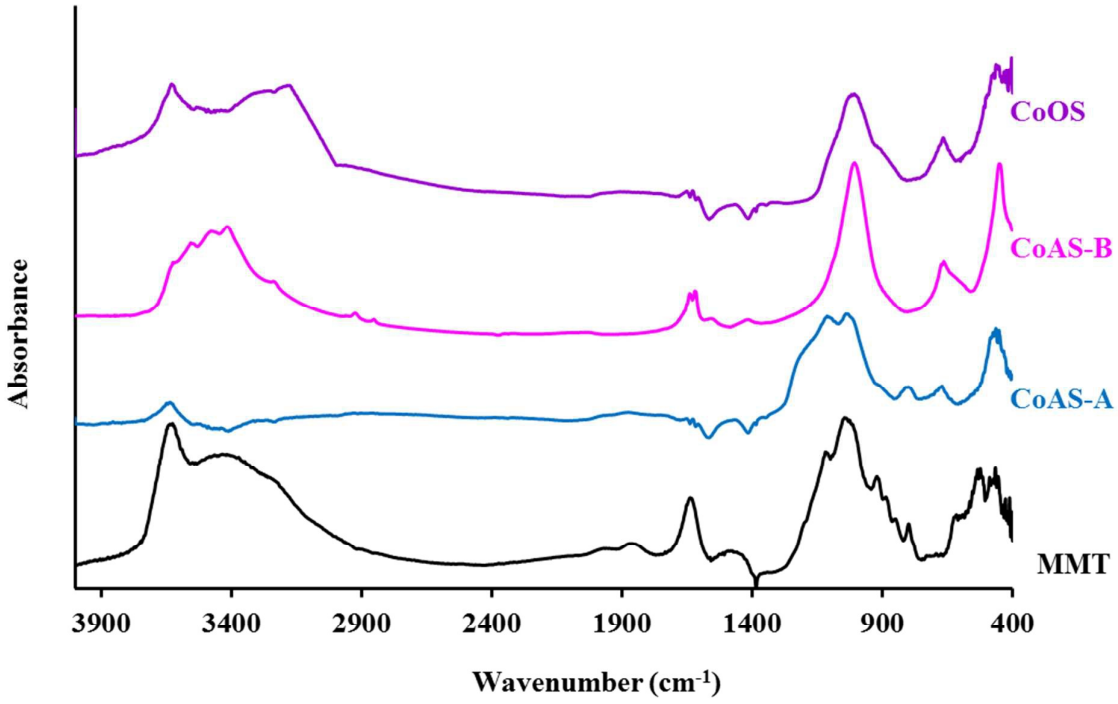

Fig. 3 FT-IR spectra for MMT and the cobalt materials.

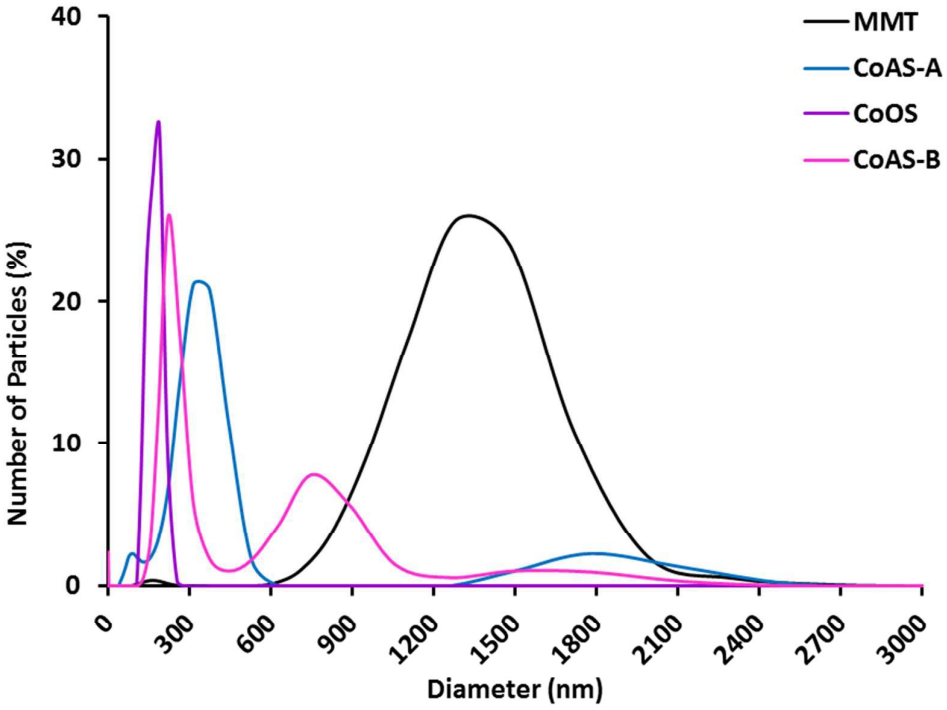

Fig. 4 Plot of number of particles (%) vs. particle size.

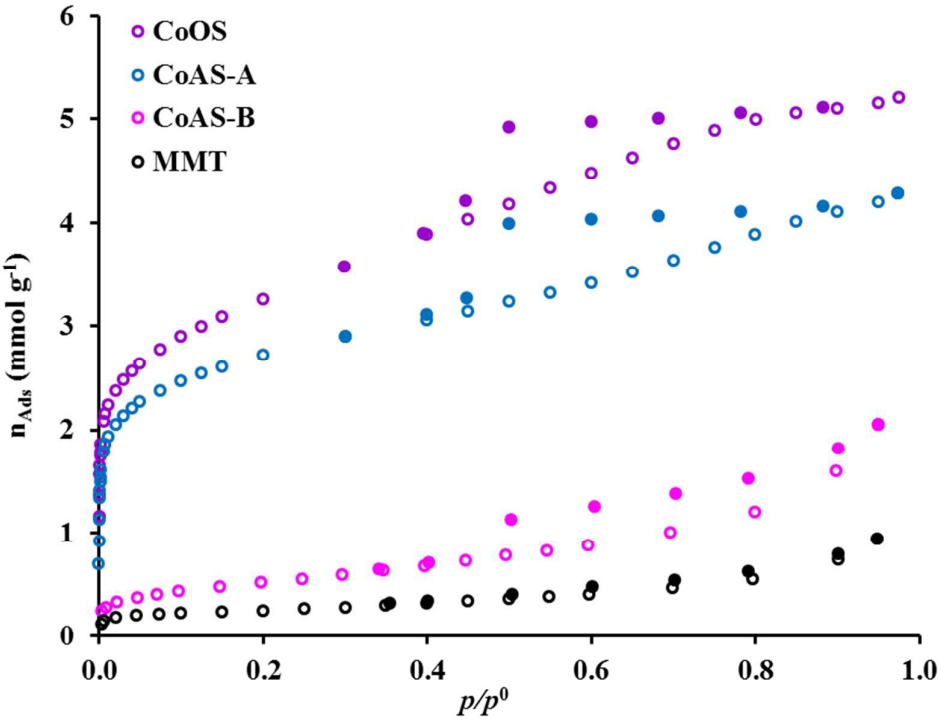

Fig. 5 Nitrogen adsorption-desorption curves at -196 ºC.

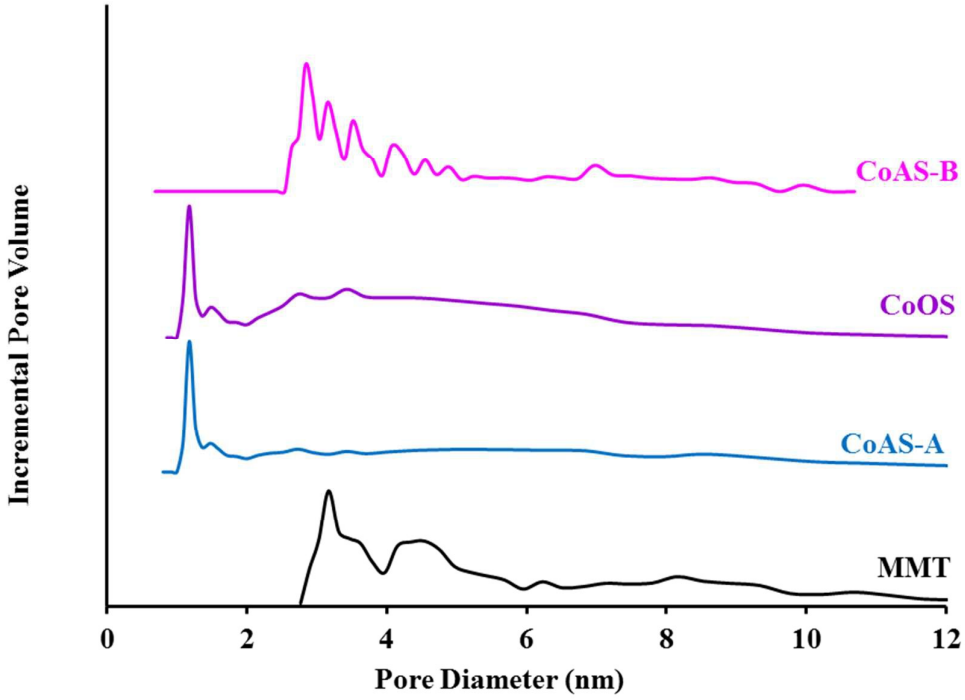

Fig. 6 Pore size distribution.

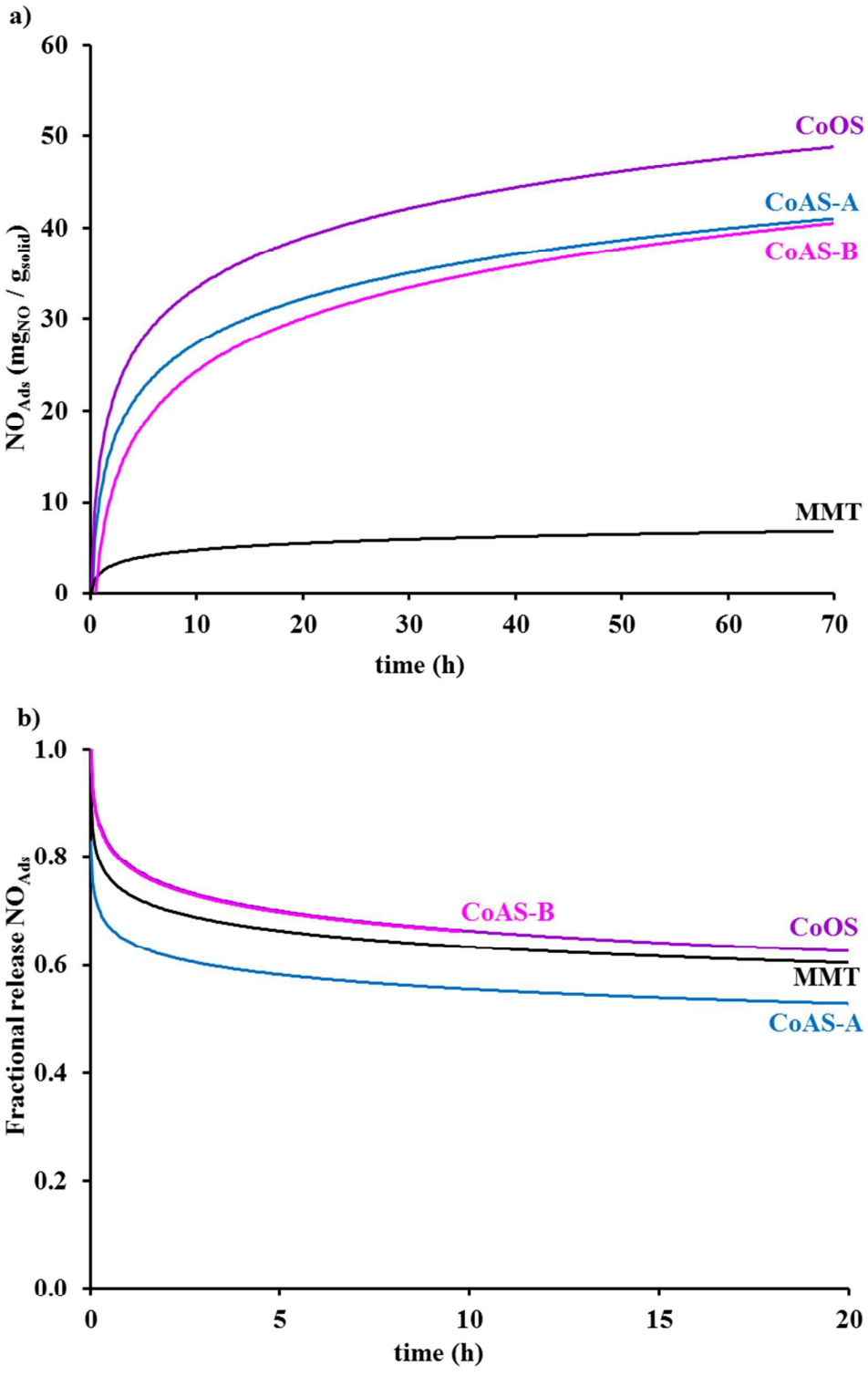

Fig. 7 Nitric oxide a) adsorption and b) release, at 25 ºC.

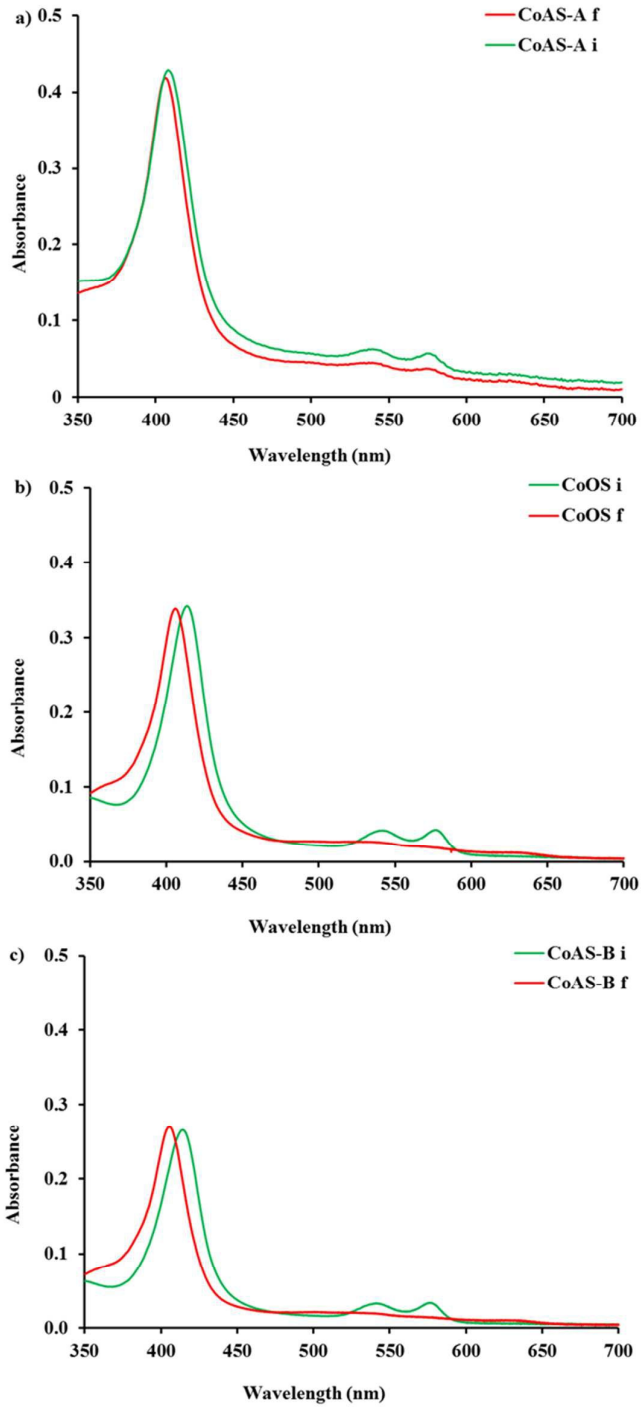

Fig. 8 Changes in the UV-Vis spectrum of the oxyhemoglobin solution upon introduction of the materials with loaded NO. a) CoAS-A, b) CoOS, c) CoAS-B. (i – initial spectrum; f – spectrum after 2 hours)

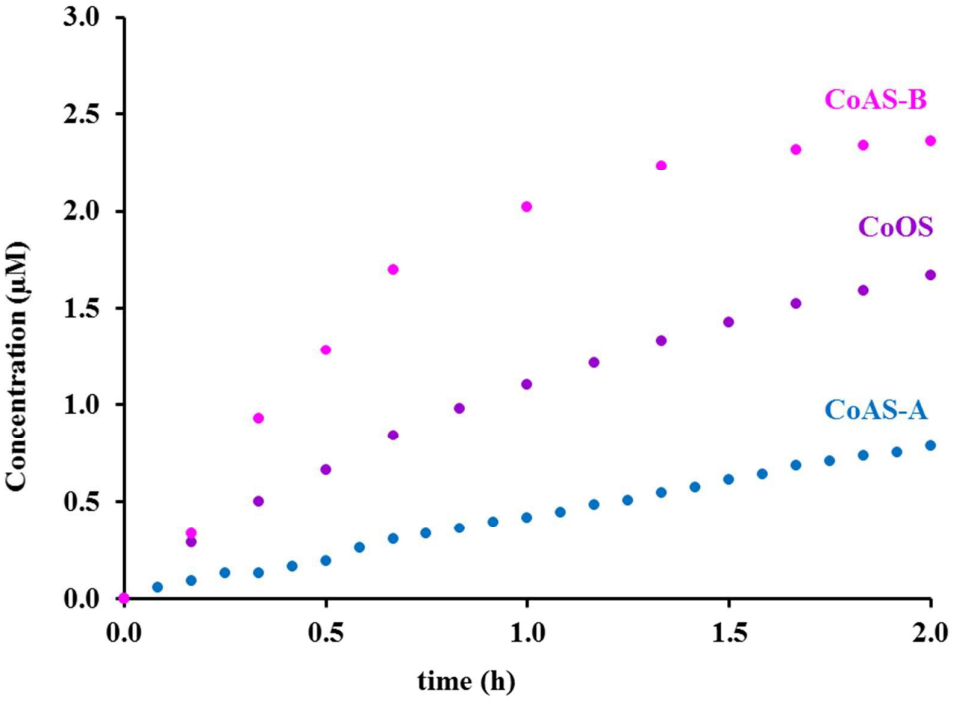

Fig. 9 Concentration of the nitric oxide released on liquid phase.

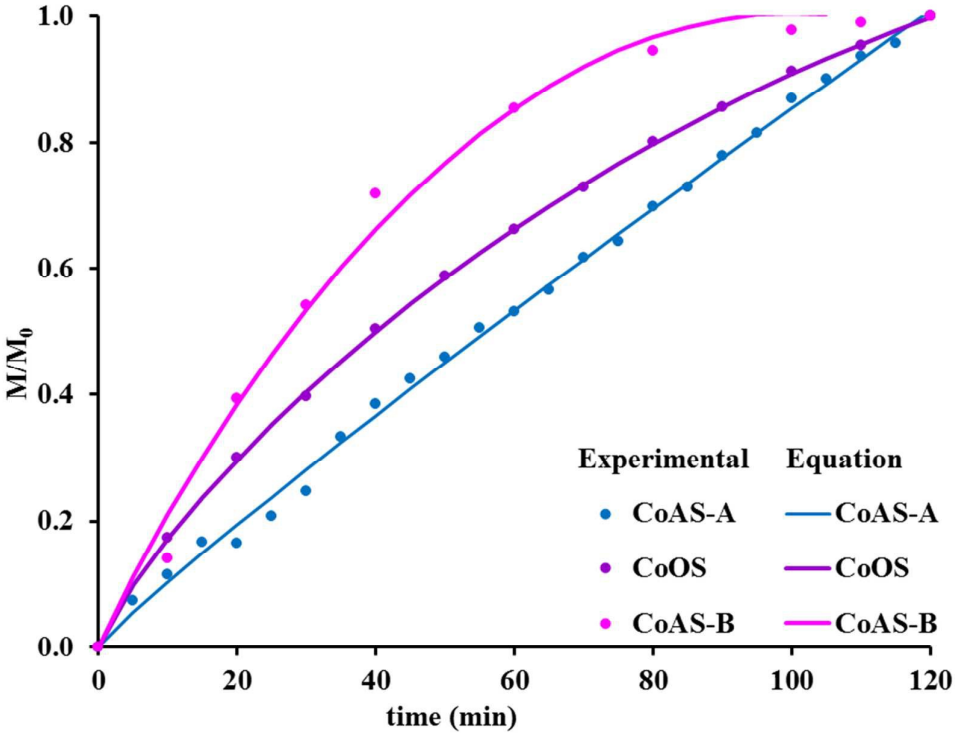

Fig. 10 NO fractional release (M/M_0) in the liquid phase. Lines are the results from the models applied.

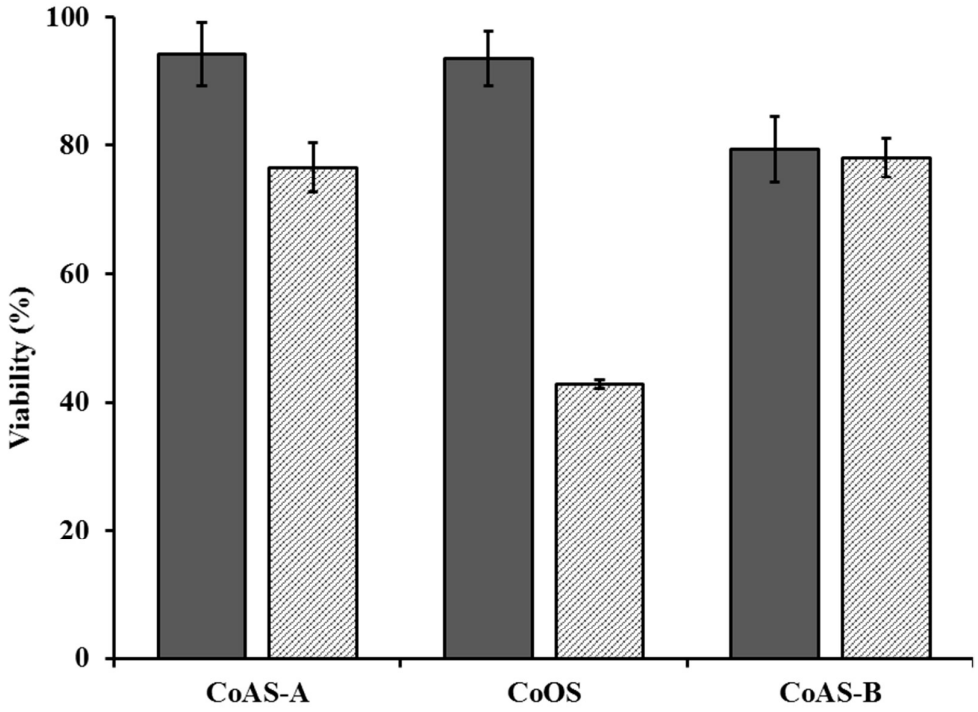

Fig. 11 Cell viability after 24 (solid) and 72h (dashed) contact with 450 µg/mL of the materials.

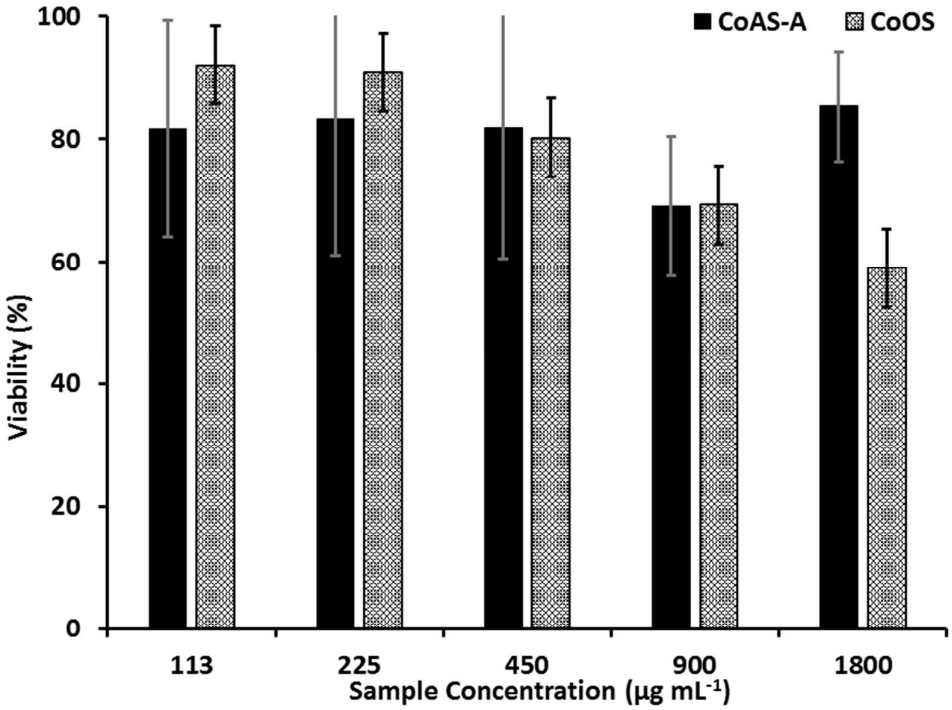

Fig. 12 Viability vs material concentration, after 24h.

Table 1

Basal spacing d_{001} for the studied samples

Material	d_{001} (Å)		
	Dry	**Glycolation**	**300 °*C***
CoSA-A	14.2	20.1	12.2
CoOS	11.9	19.5	11.2
CoSA-B	13.0	15.9	11.9
MMT	12.6	16.4	9.5

Table 2

BET surface area (A_{BET}), microporous (V_{μ}) and mesoporous (V_m) volumes for the studied samples

Material	A_{BET} (m^2g^{-1})	V_{μ} (cm^3g^{-1})	V_m (cm^3g^{-1})
MMT	20	0.007	0.391
CoSA-A	218	0.066	0.084
CoOS	246	0.035	0.125
CoSA-B	41	0.000	0.093

Table 3

Amounts of NO adsorbed and released.

Material	$\%NO_{Ads}$ [a]	NO_{Ads} [b]	NO_{Rel} [c]	NO_{Rel} [d]
MMT	0.7	7.20	2.1	2.8
CoAS-A	4.5	45.0	8.0	13.2
CoAS-B	3.5	35.0	8.5	12.0[e]
CoOS	5.1	51.0	6.9	10.2

[a] maximum NO adsorbed in gas phase, [b] maximum NO adsorbed in gas phase (mg_{NO}/g_{solid}), [c] NO released after 2h in gas phase (mg_{NO}/g_{solid}), [d]NO released after 20 h in gas phase (mg_{NO}/g_{solid}), [e] NO released after 10 h in gas phase (mg_{NO}/g_{solid}).

Table 4

NO released amounts in liquid phase after 2 hours.

Material	[NO] (μM)	[NO] ($\mu g_{NO}/g_{sample}$)
CoAS-A	0.8	16
CoAS-B	2.4	47
CoOS	1.7	33

Table 5

Results for the fitting application of the kinetic models for liquid release.

Material	Peppas-Sahlin		
	k_d	k_r	n
MMT	0.0630± 0.00400	0.0050 ± 0.00300	0.6050 ± 0.12600
CoOS	0.0260 ± 0.00100	-0.0001± 0.00001	0.8310± 0.01100
CoAS-B	0.0250± 0.00600	-0.0002± 0.00007	0.9510± 0.06100
	Korsmeyer-Peppas		
	k	**n**	
CoAS-A	$0{,}012 \pm 7{,}92\times10^{-4}$	0,922 ± 0,144	

k_d, diffusion kinetics constant from Peppas-Sahlin equation (min^{-n}); k_r, relaxation kinetics constant from Peppas-Sahlin equation (min^{-2n}); k, diffusion kinetics constant from Korsmeyer equation(min^{-n}); n, release exponent.

TOC

Synthetic cobalt clays for the storage and slow release of therapeutic nitric oxide

Ana C. Fernandes[a]*; Moisés L. Pinto*[b]*, Fernando Antunes*[a]*, João Pires*[a]

[a] Centro de Química e Bioquímica, Faculdade de Ciências, Universidade de Lisboa, 1749-016 Lisboa, Portugal

[b] CERENA, Instituto Superior Técnico, Universidade de Lisboa, Av. Rovisco Pais, nº 1, 1049-001 Lisboa, Portugal